Energy & Buildings 324 (2024) 114857

Contents lists available at ScienceDirect

Energy & Buildings

journal homepage: www.elsevier.com/locate/enb

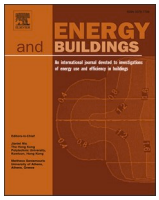

On the impact of hollow silica powder on the performance of aerogel glazing systems in buildings: Results from laboratory and simulation analyses

F. Merli [a], C. Buratti [a], T. Ihara [b], A.G. Mainini [c], A. Augello [c], M. Zinzi [d,*]

[a] Department of Engineering, University of Perugia, Via G. Duranti 63, 06125 Perugia, Italy
[b] Technology Head Department, Takenaka Corporation, Tokyo, Japan
[c] Department of Architecture, Built Environment and Construction Engineering, Politecnico di Milano, Via Ponzio 31, 20133 Milan, Italy
[d] Department of Energy Technologies and Renewable Sources, ENEA, Via Anguillarese 301, 00123 Rome, Italy

ARTICLE INFO

Keywords:
Hollow silica powder
Aerogel glazing systems
Thermal and optical properties measurements
Dynamic simulation
Energy savings

ABSTRACT

Aerogel-based glazing systems are an effective solution to reduce space heating energy use in buildings, even if overheating risks in temperate climates exist due to the high solar transparency of the systems. This study analyzes the potential of an innovative solution, based on a mixture of granular aerogel and hollow silica powder, in small concentrations, to increase the reflectance of the aerogel layer and reduce solar transmission. A set of glazing samples, different in aerogel layer and powder concentration, were produced and test in laboratory to determine the relevant solar and thermal properties. It was found that at 7.5 % powder concentration the solar and light transmittance were reduced up 0.48 and 0.45 in a 0–1 scale, respectively. Analogously, the solar and light reflectance increased up 0.49 and 0.46, respectively. The thermal resistance of the system increased up to 0.18 m^2K/W, peaking at 1.88 m^2K/W for the 34 mm aerogel layer sample. The thermo-physical properties were used as input to simulate an office building in different climatic conditions; it was found that the proposed technology ensured total energy savings for 4 % powder concentration and higher; cooling energy savings were up to 21 % and total energy savings up to 21 %.

1. Introduction

Energy savings in buildings is an important tool to face global warming, by reducing the GHG emissions in the atmosphere, given the important role that the building sector plays in the world's final energy consumption, accounting for about 36 %. The building sector is also responsible for about 55 % of the global electricity use [1].

In this context, the characteristics of the building are crucial to reduce energy use, especially when considering the transparent components: allowing natural lighting, they contribute to the reduction of energy for artificial lighting, but they also significantly contribute to increase heating and cooling loads. A correct balance between these opposite trends is necessary in the building design.

Innovative transparent solutions such as aerogel glazing systems could be able to enhance the energy performance of buildings, thanks to their high light transmission and low thermal conductivity [2].

Several studies in the Literature demonstrated the effectiveness of the use of aerogel glazing systems in cold climates, where a significant reduction of the energy use for heating can be achieved both with granular and monolithic forms as fillings in the gap of double glazing units. A reduction in the 10–40 % range can be obtained, depending on the aerogel layer thickness, the climate conditions, the window to wall ratio, the building geometry and characteristics, the boundary conditions, the granular or monolithic form of aerogels, and the simulation tool used [2–9]. In cooling dominated climate, aerogels show in general a worse behavior, especially in hot and temperate climates, where the annual reduction is lower than 20 % [4,5,10]. In some case studies, also in heating dominated climates such as in the UK, the cooling energy consumption of a guesthouse is one order of magnitude higher than the heating demand (about 35–37 % of the total energy consumption of the building for cooling versus 3–4 % for heating) [11]. In some case studies, the introduction of the aerogel in the gap lead to an increase of the

* Corresponding author.
E-mail address: michele.zinzi@enea.it (M. Zinzi).

https://doi.org/10.1016/j.enbuild.2024.114857
Received 22 July 2024; Received in revised form 13 September 2024; Accepted 28 September 2024
Available online 30 September 2024

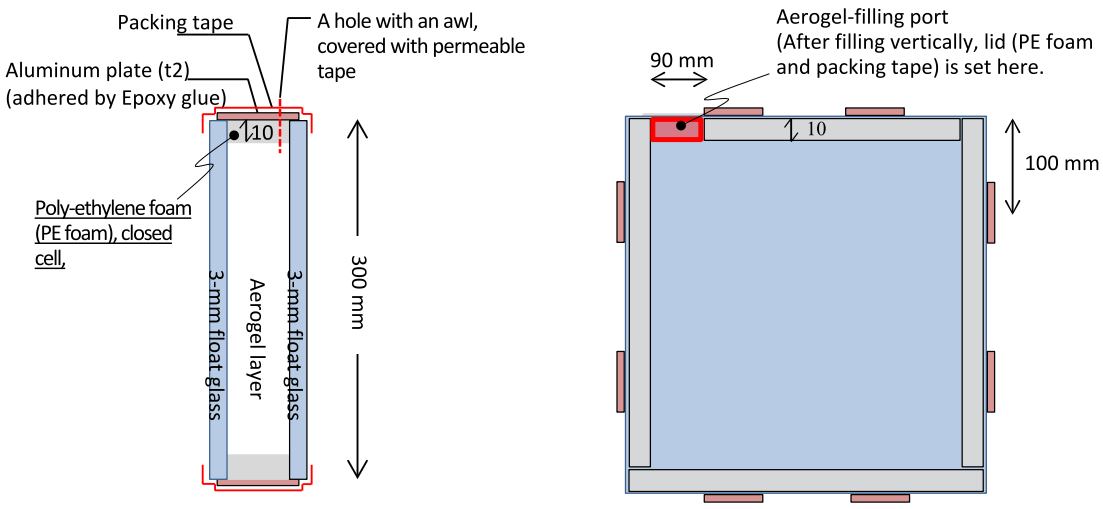

Fig. 1. Description of the assembled samples.

cooling loads [6]. It depends on the absence of robust methods to calculate the solar heat gain, on the high g-value in general estimated and used as input in the simulations [12], based on approximate methodologies, and on the overheating risk associated to un-shaded glazing systems, which play a crucial role in the calculations [2].

The reduction of solar heat gains is crucial to reduce cooling energy use and several solutions were proposed in the Literature. The most recent studies focused on the impact of fenestration and shading devices [13], advanced smart fenestration [14,15], and glass configurations [16]. In [13] the influence of fenestration and shading device (F&SD) installations on the energy performance of an office unit in a building in Shanghai was studied using brute-force parametric analysis and Monte Carlo sensitivity analysis. The investigated parameters included window-facing orientation, window-to-wall ratio, shading device types, number of shadings, shading device depths, and shading tilt angles. The results show that in summer and in winter, the highest solar heat gain (SHG) is observed when the window is West- and South-oriented, respectively. As expected, the SHG decreased with more shading devices and less window area; it can be reduced up to 93.8 % by applying F&SD, with mean values in the 40–60 %. Innovative solutions such as adaptive fenestration systems are studied in [14], where thermotropic (TT) materials and parallel slats transparent insulation materials (PS-TIM) integrated into the air cavity of double-glazing windows were combined to develop a new glazing unit. The proposed solution can offer a substantial reduction (up to 0.5) in solar transmittance transitioning from clear to translucent state, accompanied by a significant reduction in the solar factor. Based on the weather conditions of London, the TT PS-TIM system exhibits a 30 % reduction in heat gain during summer and a 20 % reduction in heat loss in winter, when compared to a conventional Double Glazing (DG) system. Smart solutions were also considered in [15], such as vacuum glass with suspended particle device and polymer dispersed liquid crystal, both able to switch between clear and translucent states. In these cases, the reference standard Double low-E coated glass proved to have the least heat gain among all the glass samples, whereas among the innovative glass options, the polymer dispersed liquid crystal glass exhibited lower heat gain compared to vacuum glass with suspended particles. Finally, in [16] different kinds of glass (laminated, heat-strengthened, tempered, and annealed) are considered in different combinations (double and triple glazing units). Results showed that the combination with the lower solar heat gain value are the double units with low-e glasses.

Low thermal transmittance and high solar gains of aerogels are indeed critical issues, which may affect the building cooling and total energy use with respect to conventional glazing systems in temperate and hot climates. Improving the solar control of aerogel based glazing units was little explored; a potential solution is represented by adding hollow silica powder to granular aerogel, as documented in preliminary studies of the Authors [17,18], and in a paper about the sound absorption of the aerogel powders [19]. However, the acoustic aspect was not addressed in this research and will represent a future development of the study.

In particular, the Authors recently developed a preliminary study with the objective of increasing the reflectance and reducing the transmittance of the transparent components. The study is focused on the thermal and optical properties of polycarbonate panels with granular aerogel and two different diameters of silica powder (0.3 mm and 0.05 mm), considering different thicknesses and percentages. Given the diffusive nature of the material and the scattering, the optical performance was investigated with a large sphere spectrophotometer, and the thermal performance with a guarded hot-plate facility. Thermal performance improves with powder content and thickness of the panel (thermal transmittance U-values in the 3.25–0.61 W/m^{2}K range for a single polycarbonate layer with powder and 27-mm package with granular aerogel and powder). At the same time, a reduction of optical transmission is found when increasing powder content and thickness (light transmittance in the 0.5–0.09 range). A reduction of the solar transmittance up to 80 % with respect to the same sample without the powder is also obtained for the thicker panel with 7 % vol. of powder [17]. In a previous study [18], the same Authors investigated the behavior of a double glazing system with a 24-mm layer of silica aerogel and a few weight percentages of hollow powder. The investigated sample showed a U-value of 0.7 W/m^{2}K and a visible and solar transmittance of 0.35 and 0.28, respectively. A simulation model of an office sited in Tokyo (Japan) showed that the addition of the powder in the granular aerogel produces a reduction of the cooling energy demand in the 14–24 % range, depending on the wall facing, with a low cost of the powder addition, resulting in a short Pay – Back period (2–7 years) [14].

Starting from the above described background, the present study aims to systematically investigate the impact of silica powder on the thermal and optical properties of granular aerogel double glazing unit doped with silica power by experimental analysis; next, the impact on the total energy performance of a reference building under different climate conditions is assessed through simulations in dynamic regime. The ultimate objective is to demonstrate whether the use of silica powder can improve the performance of conventional aerogel glazing by reducing the solar gains in buildings with high cooling demand,

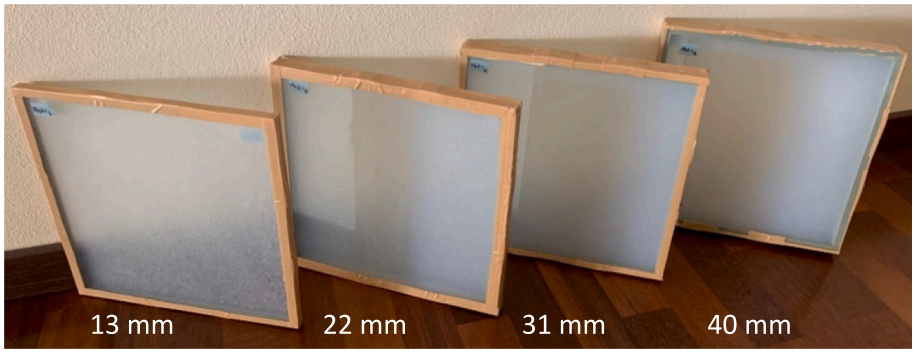

Fig. 2. The investigated samples: glazing systems with 1% silica powder at different thicknesses.

Table 1
Samples characteristics.

Sample ID	Gap [mm]	Total thickness [mm]	Powder [%]	Sample ID	Gap [mm]	Total thickness [mm]	Powder [%]
2-1	7	13	0.0	4-1	25	31	0.0
2-2	7		1.0	4-2	25		1.0
2-3	7		2.0	4-3	25		2.0
2-4	7		4.0	4-4	25		4.0
2-5	7		7.5	4-5	25		7.5
3-1	16	22	0.0	5-1	34	40	0.0
3-2	16		1.0	5-2	34		1.0
3-3	16		2.0	5-3	34		2.0
3-4	16		4.0	5-4	34		4.0
3-5	16		7.5	5-5	34		7.5

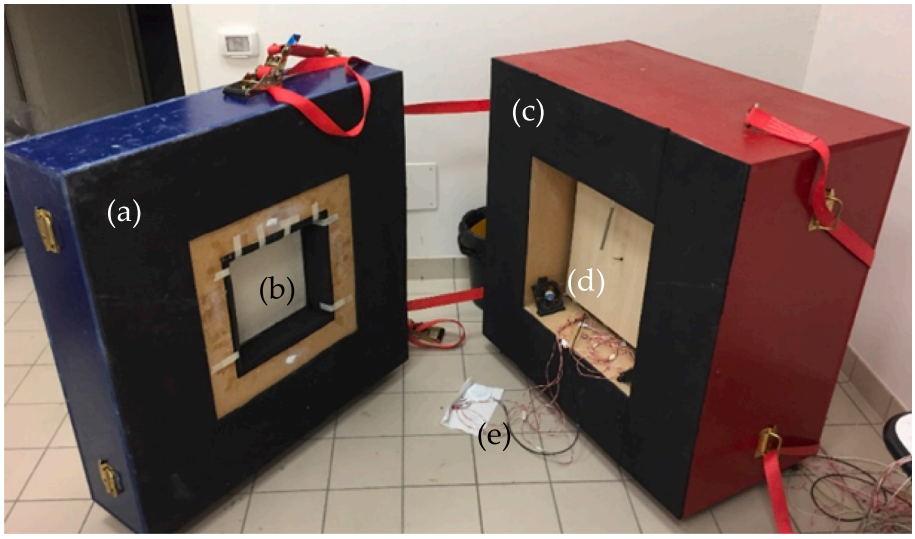

Fig. 3. Small Hot Box apparatus: sample holder compartment (a); sample (b); hot chamber (c); radiative panel (d); thermoreristances and thermal flux meter probes (e).

Table 2
Weather locations selected.

Country	City	Location	Latitude	Longitude	Koppen-Geiger Classification
Finland	Helsinki	Airport	60.32	24.97	Dfb
France	Paris	Montsouris	48.82	2.33	Cfb
Italy	Palermo	B. Di Falco	38.12	13.32	Csa

covering the current research gap. In addition, by calculating heating, cooling, and artificial lighting energy consumption, it is possible to provide initial data about the trade-off between cooling load reduction and electric lighting increase, thanks to the change of aerogel visible and solar transmittance when the silica powder is introduced in the mixture.

2. Experimental campaigns

To preserve the insulating properties of aerogel while improving the solar control of the glazing systems based on this material, the study focuses on the development of a mixture of granular aerogel and silica powder to be used in the gap of double (or multiple) glazing units. The study combines experimental and numerical analyses in an attempt of a complete assessment, from the component characterization to the building integration potential.

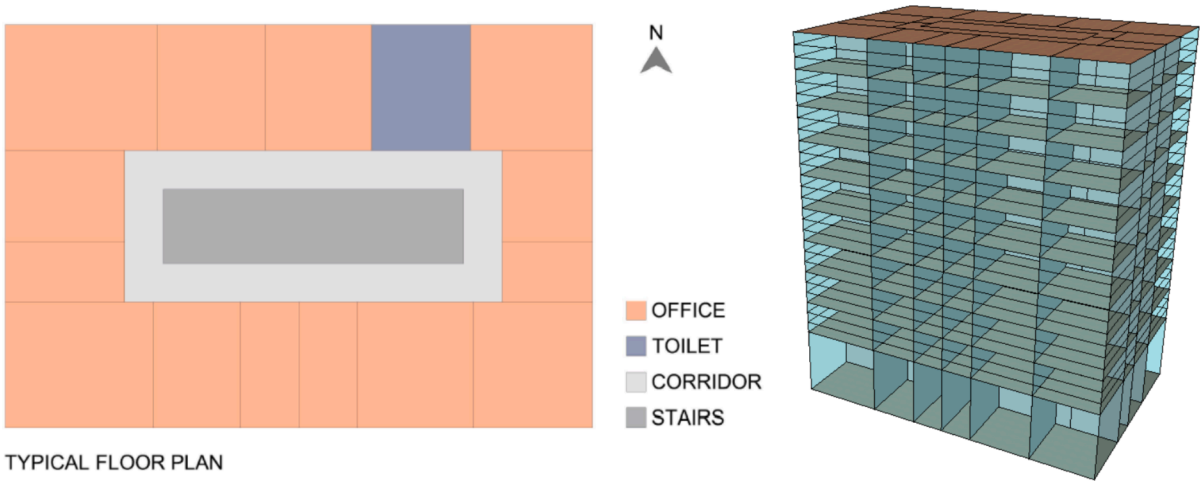

Fig. 4. Schematic plan view of the building with indication of the room typologies (left); General view of the building (right).

Table 3
Main characteristic of the opaque and transparent envelope components.

Opaque envelope component	Thickness [m]	Thermal transmittance – U-value [W/m^{2}K]
Roof	0.253	0.19
Internal floor	0.283	1.09
Internal partition	0.075	1.79
External wall	0.330	0.30
Ground exposed floor	0.230	0.33

Transparent envelope component	Frame thermal resistance R_{frame} [m^{2}K/W]	Frame factor [-]	Solar factor g-value [-]	τ_v [-]	Thermal transmittance U-value [W/m^{2}K]
External glazing (middle band)	0.5	0.85	0.29	0.75	1.07

The methodological framework is following described:

i. definition of base products and of the glazing system configurations;
ii. sample set preparation;
iii. optical and thermal characterization of the sample set;
iv. numerical assessment of the total energy use (heating, cooling, and lighting) of a reference building equipped with the selected aerogel glazing units.

Since the numerical and experimental findings, the performance of enhanced solar-control aerogel glazing systems are presented and discussed, compared to previous studies on conventional aerogel solutions.

2.1. Sample preparation

The double glazing units (DGU) were assembled by Takenaka Corporation, as detailed in Fig. 1. Each sample is 30 × 30 cm^2 and it is made with two 3-mm thick float glasses (sample ID 1), assembled in different gap thicknesses (7 mm, 16 mm, 25 mm, and 34 mm), as shown in Fig. 2. The gap is filled with a mixture of granular aerogel and hollow silica powder, the latter in different weight percentages (0.0, 1.0, 2.0, 4.0, 7.5).

The cavity is filled up vertically by means of a filling port in a very accurate way to avoid the drop of the filling and the breaking of the granules; then the aerogel double glazing unit is sealed with tape. Table 1 shows the samples identification code and the main characteristics of the tested configurations.

2.2. Optical characterization

Conventional spectrophotometers are not suitable for measuring the optical properties of granular aerogel systems, due to their geometric complexity and scattering behaviour of aerogel [2]. An in-house apparatus was then used for the purpose, whose general set-up, even if updated through the years, can be found in [20]. It is an experimental spectrophotometer equipped with a 75 cm diameter integrating sphere, which allows measurements on complex samples at normal and off-normal incidence. The integrating sphere structure is made of aluminium shell, which on the internal side has a layer of Spectralon characterized by high reflectivity and diffusing behaviour across the whole solar spectrum. The sphere has several ports used to place the light source, the sample, and the correction with the auxiliary lamp method, needed for a single beam spectrophotometer. The sample port is 20 cm in diameter, suitable for the complex samples under examination.

Measurements are carried out using two light sources. The 300 W Xenon arc lamp covers about the 300–1000 nm range, which includes part of UV, all the visible spectrum, and a portion of the near-infrared. The power tunable 1000 W tungsten halogen lamp covers the 500–2300 nm range, which covers part of the visible and almost all the near-infrared spectrum; according to standards [21], the solar range extends from 300 to 2500 nm, but after 2300 only a residual part of the spectrum power falls in. The two sources are of the “white” light type; they are collimated, but the size of the incident light beam can be changed using lenses and diaphragms mounted in series to the lamps. The detection system is made of a diode array, equipped with three sensors: the NMOS (N-type Metal Oxide Semiconductor, 250–1000 nm) covers the visible range, the InGaAs (Indium Gallium Arsenide,

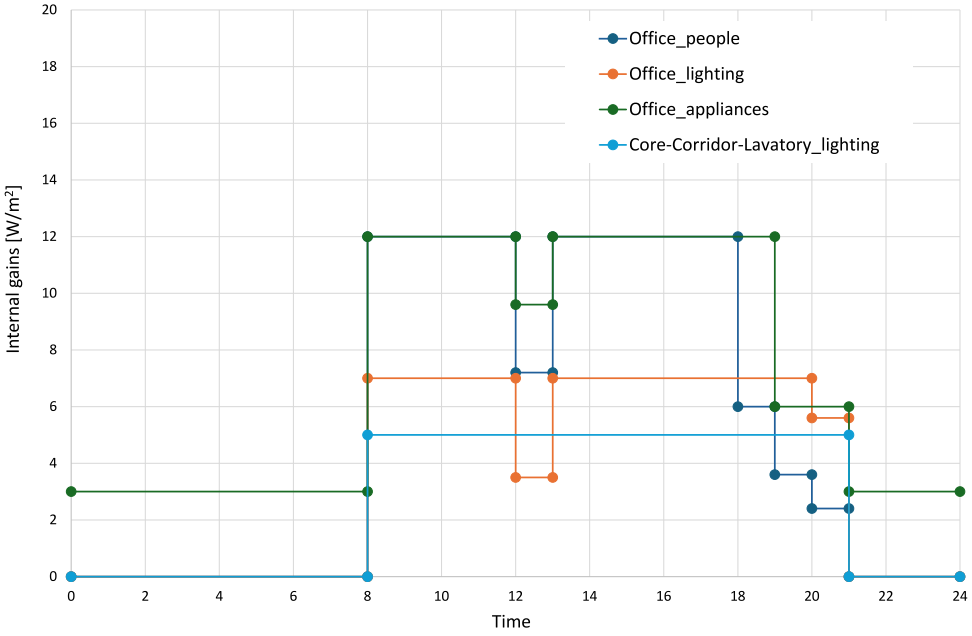

Fig. 5. Hourly Internal gains profiles per room typology.

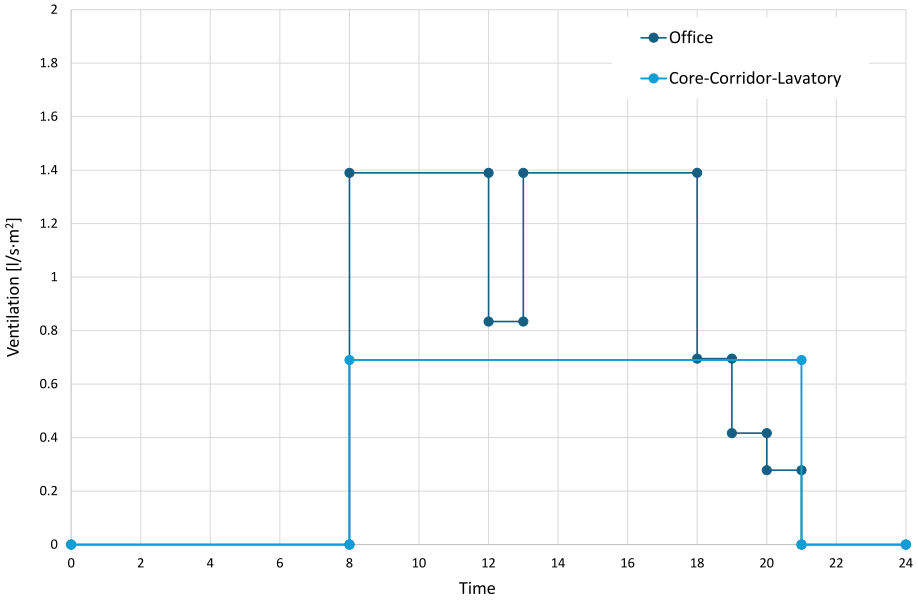

Fig. 6. Hourly Ventilation profiles per room typology.

Table 4
Heating and cooling capacity for the selected climates.

Climate	Heating capacity [kW]	Cooling capacity [kW]
Helsinki	46	48
Paris	18	48
Palermo	2	67

900–2100) covers most of the near-infrared region, and the ExtInGaAs covers the remaining wavelengths until 2300 nm.

The incident beam diameter was set to 60 mm for this experimental study, so as to have an irradiated area of about 30 cm^2 (conventional spectrophotometer beams are about 1 cm^2), suitable for this experimental campaign. Reflectance measurements were carried out at normal incidence; transmittance measurements were carried out at normal incidence for all the samples; for selected ones measurements were performed also at off-normal incidence, specifically at 0°, 30°, 45°, 60° incidence angles.

The raw spectral data are post-processed by cubic interpolation, so as to have 1-nm spectral resolution in the final measurement dataset.

The relative reflectance measurements were carried out against a white Spectralon calibrated reference, whereas the absolute transmittance measurements were against the void (empty sample port). The measurement uncertainty is ±0.02 in the 0–1 range of the measured quantity. For this experiment, measurements were performed between 350 nm and 2300 nm, covering 98 % of the solar spectrum power.

To investigate the scattering behaviour of the samples and to provide a characterization using a standard instrument, measurements were also carried out with a commercial spectrophotometer. Normal incidence – hemispherical transmittance and near-normal – hemispherical

Table 5
Broad-band optical parameters calculated for all the glazing unit configurations.

Sample	τ_v [-]	τ_e [-]	ρ_v [-]	ρ_e [-]	Sample	τ_v [-]	τ_e [-]	ρ_v [-]	ρ_e [-]
2-1	0.79	0.73	0.19	0.18	4-1	0.65	0.59	0.30	0.26
2-2	0.73	0.67	0.26	0.24	4-2	0.49	0.44	0.49	0.44
2-3	0.67	0.61	0.33	0.30	4-3	0.40	0.35	0.58	0.53
2-4	0.57	0.52	0.43	0.40	4-4	0.28	0.25	0.70	0.65
2-5	0.41	0.37	0.56	0.53	4-5	0.19	0.16	0.79	0.72
3-1	0.73	0.67	0.25	0.22	5-1	0.58	0.53	0.35	0.30
3-2	0.58	0.53	0.41	0.37	5-2	0.41	0.37	0.54	0.49
3-3	0.50	0.45	0.49	0.45	5-3	0.32	0.28	0.65	0.59
3-4	0.38	0.34	0.62	0.57	5-4	0.23	0.19	0.75	0.69
3-5	0.25	0.22	0.73	0.67	5-5	0.14	0.12	0.83	0.76

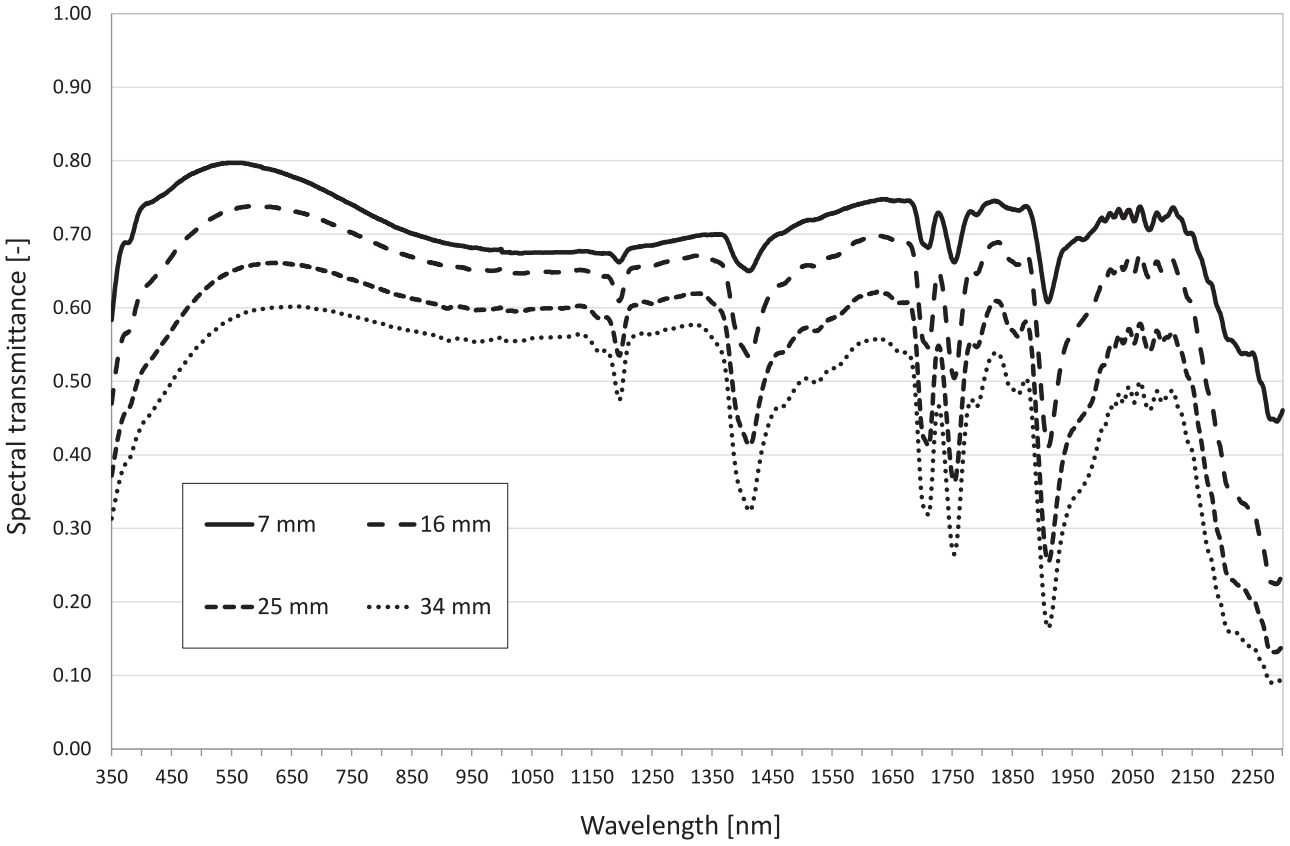

Fig. 7. Normal spectral transmittance of the aerogel samples without silica powder added.

reflectance measurements were carried out with a Perkin Elmer Lambda 950, a double beam spectrophotometer equipped with a 15 cm Spectralon coated integrating sphere. The measurements were performed on three different spots on the sample, to assess the uniformity of the aerogel glazing's optical properties. Spectral resolution was set to 5 nm and the slit width was 2 nm in UV–visible range and in auto-servo mode in the near-infrared region (this operation mode automatically sets the slit width of the instrument as a function of the radiant power in the measurement wavelength). Measurements were performed in the 300–2500 nm range, corresponding to the solar spectrum as defined in the standard EN 410:2011 [21].

The light and direct solar reflectance and transmittance were calculated from the spectral measurements resulting from both the in house made and the conventional spectrophotometers, using a weighted average across the solar spectrum, following the procedure in the EN 410 Standard [21].

2.3. Thermal characterization

The thermal resistance of the selected samples was measured by using the Small Hot Box experimental apparatus (Fig. 3) [22]. It consists of a hot chamber with external dimensions of 0.94x0.94x0.50 m (inside volume of 0.073 m^3), built with insulating materials, to minimize the heat flow through the walls. The chamber is equipped with a heating cable (maximum output power 50 W); it allows to perform tests with a minimum temperature difference of 20 °C, in compliance with the EN ISO 8990:1996 standard [23]. A sheet of plywood (radiative panel) is placed between the heating cable and the actual chamber, to avoid the radiation heat exchanges with the cable. A layered structure (2 wooden panels with an intermediate layer of expanded polyurethane) represents the closing side of the instrument: in the central part, there is an opening for positioning the square sample (30x30 cm^2). The cold side of the system is the laboratory environment, completely isolated from the outside and kept at a constant temperature by HVAC system of the building. Tests were carried out in steady-state conditions with the

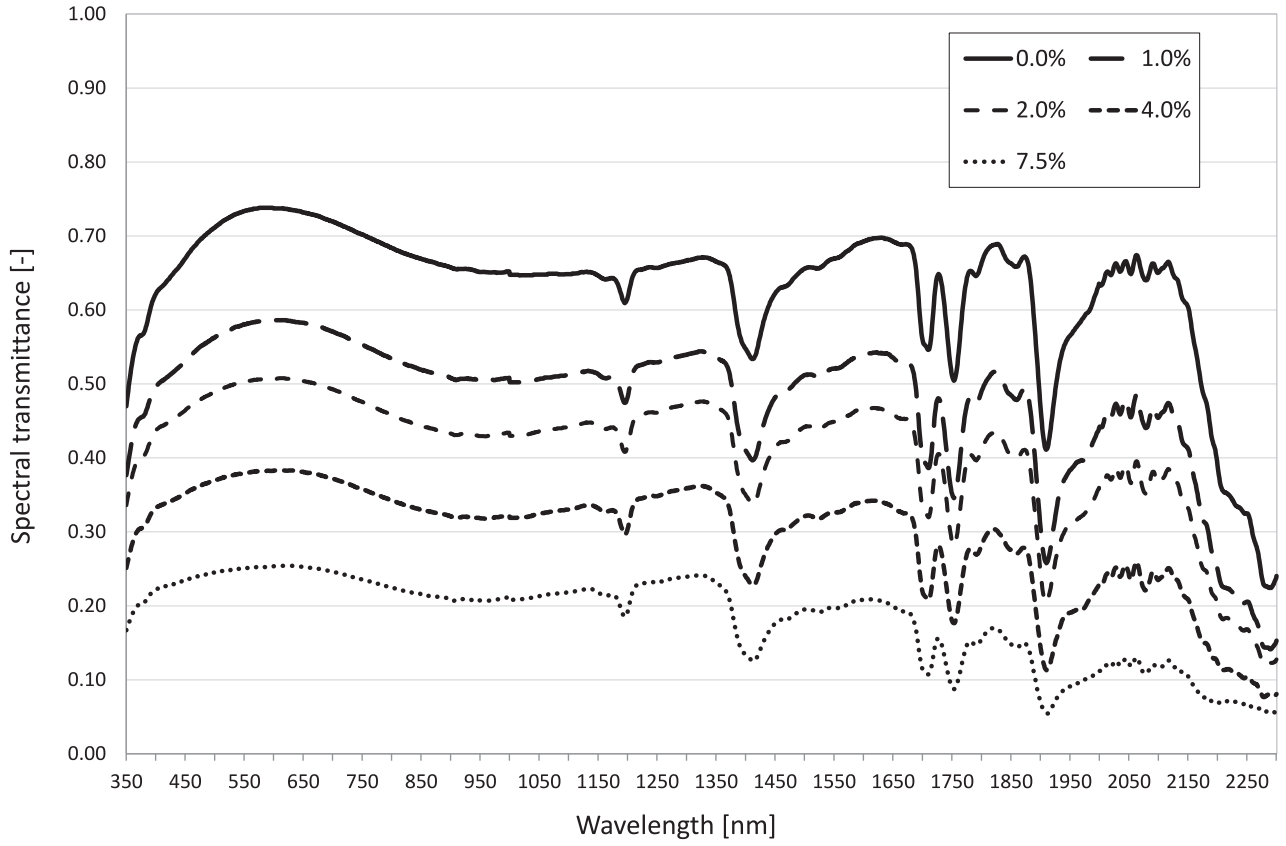

Fig. 8. Normal spectral transmittance of the 16 mm gap aerogel samples with different silica powder concentration.

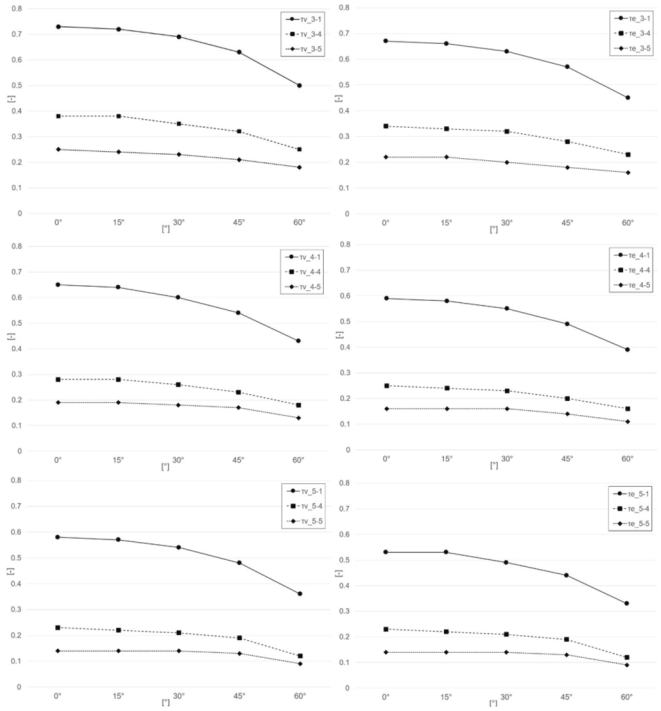

Fig. 9. Visible (left) and solar (right) angular transmittance of samples 3, 4, and 5 (top down) for three powder concentration (0%, 4%, 7.5%).

thermal flux meter method, by measuring the heat flux Φ through the sample and the mean values of the specimen surface temperatures ΔT_{sup} on the cold and hot sides. Data were measured at an average temperature of the sample in the 33–37 °C range, due to the operation conditions allowed by the test facility. To compare the performance of the investigated samples to those of conventional glazing units, the experimental data were scaled to the standard temperature of 10 °C, according to ISO 10456 standard [24].

For each aerogel sample, the experimental and post-processing procedure was as follows:

- measurement of the thermal resistance of assembled aerogel double glazing units, as shown in (1):

$$R_{tot} = \frac{\Delta T}{\Phi} \tag{1}$$

where ΔT is the difference of the mean surface temperatures of the hot and cold sides during the tests and Φ is the thermal flux measured by the thermal flux meter;

- subtraction of the contribution of the 2 glasses (t_g = 3-mm is the thickness of each glass pane) to the DGU thermal resistance, assuming 1 W/mK thermal conductivity for standard silica glass sheets λ_g, thus obtaining the thermal conductivity of the gap layer λ_a (granular aerogel/granular aerogel + hollow silica, with t_a the thickness of the gap), as (2);

$$\lambda_a = \frac{t_a}{R_{tot} - 2 \bullet \frac{t_g}{\lambda_g}} \tag{2}$$

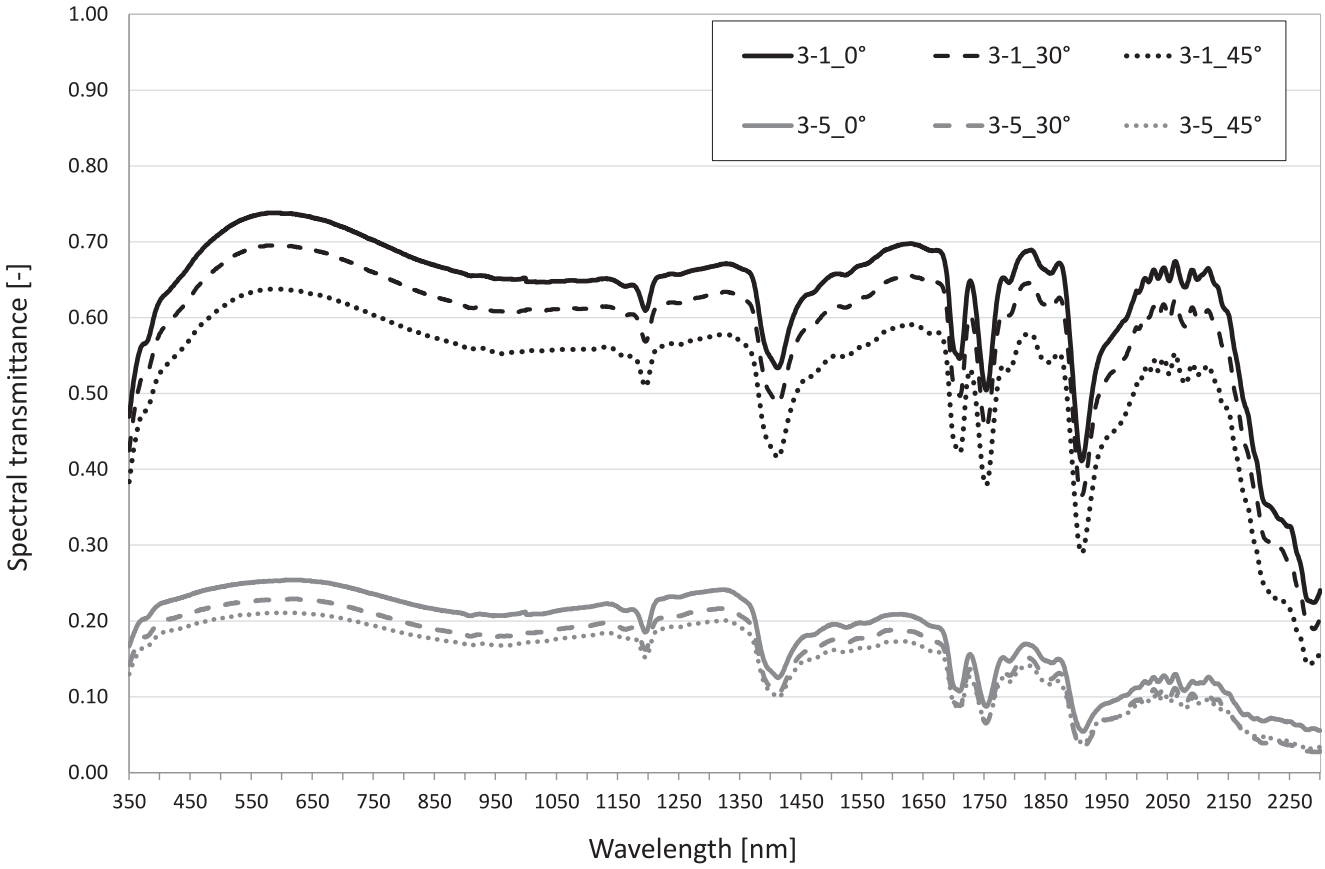

Fig. 10. Angular spectral transmittance of the 16 mm gap aerogel samples with 0 and 7.5 % silica powder concentration.

Table 6
Thermal measurements results.

sample	$R_{@10°C}$ [m²K/W]	$U_{@10°C}$ [W/m²K]	sample	$R_{@10°C}$ [m²K/W]	$U_{@10°C}$ [W/m²K]	sample	$R_{@10°C}$ [m²K/W]	$U_{@10°C}$ [W/m²K]
3-1	0.79	1.04	4-1	1.22	0.72	5-1	1.70	0.53
3-3	0.80	1.03	4-3	1.22	0.72	5-3	1.73	0.53
3-4	0.85	0.97	4-4	1.30	0.68	5-4	1.77	0.52
3-5	0.92	0.92	4-5	1.39	0.64	5-5	1.88	0.49

- λ_a was reported at a standard temperature of 10 °C $\lambda_{a@10°C}$ following the standard [24] and assuming a temperature conversion coefficient equal to 0.0052, obtained the measurements on the same aerogel granules in a previous work [25];
- thermal transmittance U of each sample was calculated as (3):

$$U = \frac{1}{R_{sup,i} + R_{tot} + R_{sup,o}} \tag{3}$$

considering the inside surface thermal resistance $R_{sup,i}$ and the outside surface thermal resistance $R_{sup,o}$ equal to 0.04 and 0.13 m^2K/W respectively, in compliance with EN 6946 standard [26].

Finally, the relative uncertainties (type B) of the tests $\dot{u}$ (R) were calculated according to JCGM 100:2008 [27].

3. Numerical analysis

To assess the performance of the analyzed technologies, dynamic energy simulations are conducted using Integrated Environmental Solutions Virtual Environment (IESVE) [28]. This software enables the evaluation and optimization of both energy and lighting performance, leveraging its native integration of the LBNL Radiance tool.

Among the possible alternatives, the samples with gap thicknesses of 16 and 25 mm are selected, as representative of the most commonly used type of double glazing systems in the construction industry. The selection includes samples with 0 %, 2 %, 4 %, and 7.5 % of powder in the aerogel mixture. This choice is made to observe a gradual variation in performance and to adequately demonstrate the potential of the proposed technology. Starting from the measured visual, solar, and thermal characteristics of the samples, the solar factor was calculated according to EN 410 [21]. The aerogel glazing units are considered as diffusing in transmission and reflection modes, thus the trans type of material was selected for lighting analyses with Radiance [29].

Climate-Based Daylight Modelling (CBDM) methods were used to create daylight coefficients for sensor or grid points; the same coefficients were then used to calculate illuminance at each time step [30]. Sensors were placed at a work-plane height of 0.78 m in the middle of each space. Daylighting analysis was then used to optimize the dimming profiles of the artificial lighting systems.

The building selected as a case study is a 10-story office building, whose typical floor has a conditioned heated area of 443.3 m^2 and an internal height of 3.3 m. It is ideally located in three significantly different climates, listed in Table 2, representing Northern, Central, and Southern Europe. All climatic data in *.EPW format is obtained using METEONORM Version 8.0.3.15910 [31].

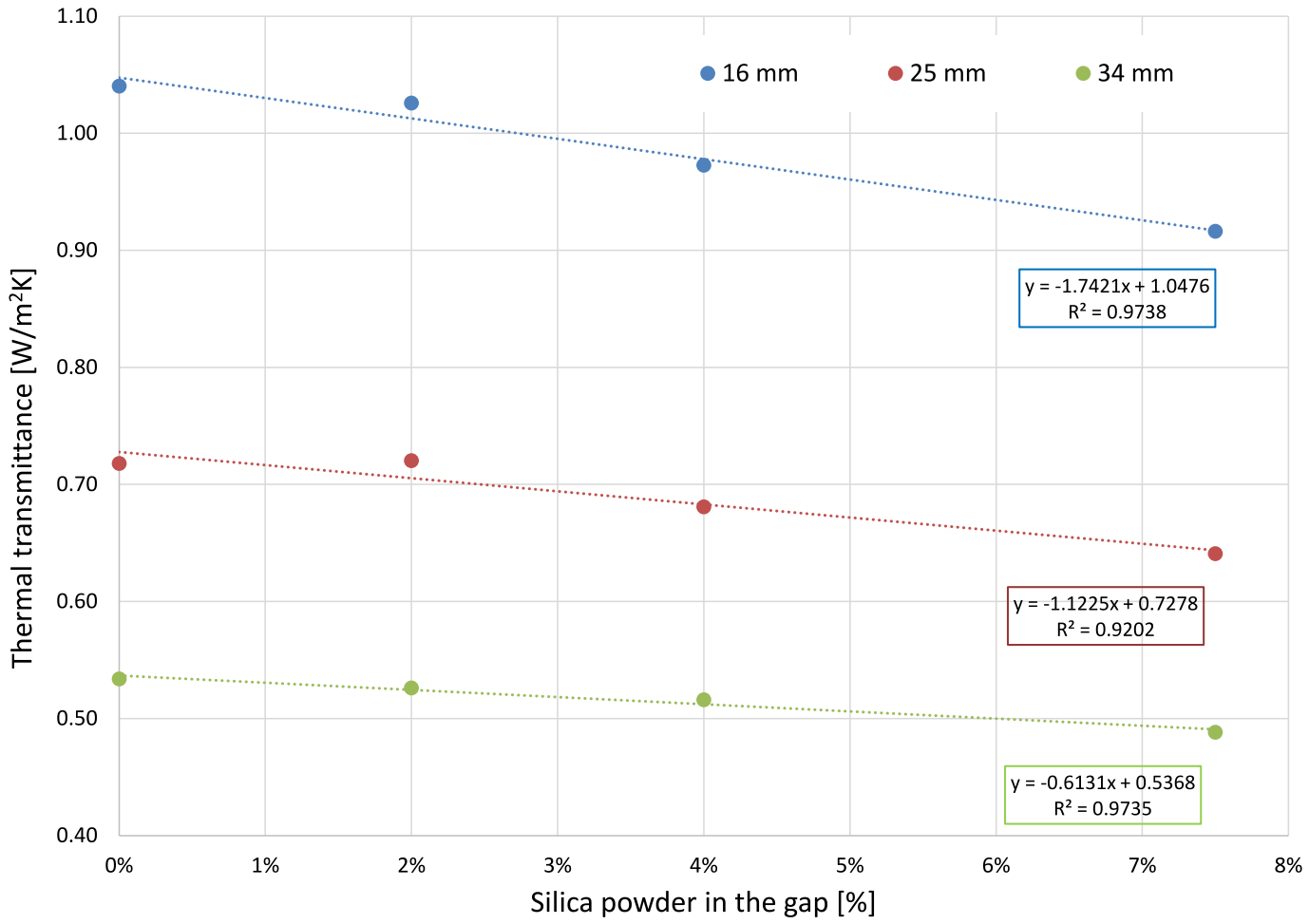

Fig. 11. Thermal transmittance values vs. percentage of silica powder in the gap.

The typical intermediate floor (Fig. 4) selected for the study consists of a central staircase surrounded by a corridor connecting 14 individual offices and a lavatory; the building's façades are fully glazed, divided into three horizontal bands of 1.1 m high each. The upper and lower bands are equipped with aerogel glazing systems, the middle band is equipped with a conventional selective low-emittance double glazing unit. The performance of the building's envelope components is reported in Table 3.

Based on ISO 18523-1:2016 [32], Figs. 5 and 6 show the values of internal gains and ventilation rates set in the model during weekdays. During the weekend, no internal gains are considered, except those related to the equipment, which has a reduced hourly constant power equal to 3 W/m^2. The infiltration rate is set at 0.1 ACH (Fig. 5). Dimmer switches are set-on to modulate the lighting system in the office areas; the system activates when there is an illuminance level below 300 lx, as measured by a sensor placed in the centre of the room during the building's normal operating hours (from 8 a.m. to 9p.m.).

The air-conditioning system consists of a reversible heat pump with fan coils serving only the office zones. The model systems were sized using the starting envelope configuration and based on the peak hourly net energy demand increased by 20 percent (Table 4); temperatures of 20 °C and 26 °C are adopted as winter and summer setpoints, respectively, with a control on indoor relative humidity with an upper limit of 55 %.

4. Results

4.1. Optical properties

Table 5 presents the broad-band values of the transmittance (τ) at normal incidence and the reflectance (ρ) at near-normal incidence, referring to the solar (subscript *e*) and visible range (subscript *v*). The float glass was measured as well and literature values were confirmed (0.91 and 0.87 for the visible and solar transmittance, respectively, and 0.08 for the reflectance in both ranges). The light and solar normal transmittance is always above 0.50 for the aerogel samples with no powder inside, conversely, the reflectance is always below 0.3, except for the thickest samples, for which 0.35 is measured. The transmittance spectra of the base-case systems are reported in Fig. 7, whereas Fig. 8 shows the plot of the spectral transmittance for the 16 mm gap sample for the different powder concentrations in, which reports.

The thin sample 2–1 (7 mm gap) has high transparency and even with the highest powder concentration (2–5 case) the solar and visible transmittance are still moderately high (around 40 %). However, to ensure higher thermal performance complying with regulatory requirements, glazing systems with such low air gap thickness are in general not used.

A different behaviour can be observed for the samples with higher thickness; the transmittance drops to about 0.50 already with 2 % powder concentration for the 16 mm gap system (3–3 case); the solar transmittance reaches 0.22 with the highest powder concentration, exhibiting high potential for solar control (3–5 case). Similar values are achieved with a 4 % concentration for the 4.4 sample (25 mm thickness):

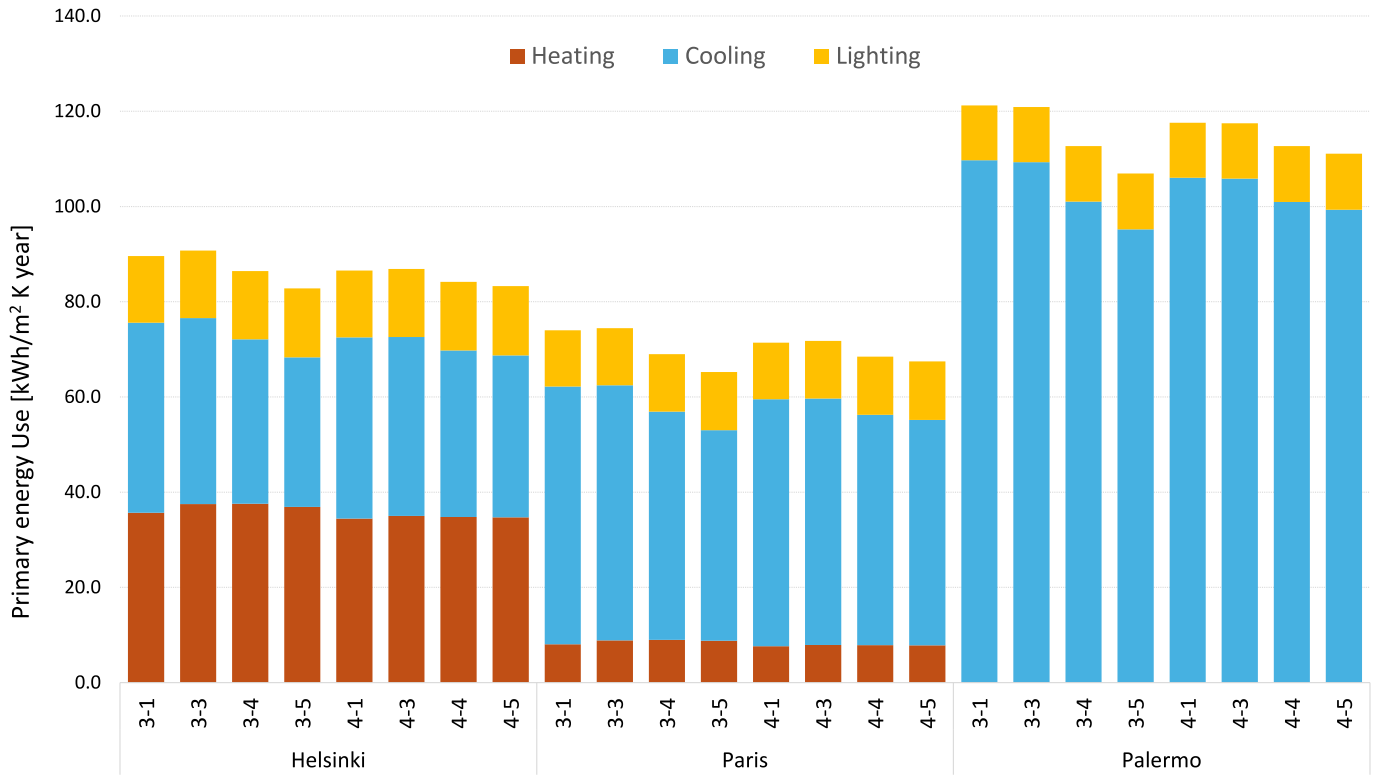

Fig. 12. Annual Primary Energy Use for Cooling, Heating, and Lighting. The results are arranged per window component typology and location.

increasing the silica powder brings the light transmittance below 0.20, in line with old tinted glasses characterized by poor daylighting. The thickest unit (34 mm) almost halves the solar transmittance with 2 % powder, scoring 0.28 (5–3 case); further increasing the amount of powder would lead to too low visible transmittance values, ranging from 0.23 (5–4 case) to 0.14 (5–5 case).

The change in transmittance is balanced by the increase in reflectance; taking as example the solar reflectance values, it can be observed that it triplicates for samples 2, 3, and 4, and it increases by 2.5 factor for sample 5. A similar trend with the smaller absolute difference is found for the light reflectance.

The angular decay of solar and light transmittance of samples 3, 4, and 5 is reported in Fig. 9. The angular decay in transmission mode is very similar for samples 3 and 4 without powder with respect to the normal incidence condition: the loss in transmittance at 45 °C is 0.1 in both cases, and it rises to 0.22–0.23 at 60°; thus, no specific trend is identified as a function of the gap thickness. Conversely, increasing the powder concentration, it is observed that the transmittance drop depends also on the sample thickness: the transmittance drops by 0.06, 0.05, and 0.04 with concentration 4 % for samples 3, 4, and 5, respectively, at 45°; for the same concentration, at 60° the transmittance reduction is 0.13 for sample 3 and 0.11 for sample 4 and 5. The trends are confirmed for the concentration of 7.5 % at 45°, as well as for the measurements at 60°. The results also highlight similar relative variations at 45° and 60° for all the configurations, except for the thickest sample with the highest concentration, whose variation at 45° is only 7 %, whereas in all the other cases it is 14–17 %. At 60°, the relative variations are all in the 32–38 % range, with respect to the normal incidence condition.

As an exemplary case, Fig. 10 shows the spectral transmittance at 0°, 30°, and 60° incidence angle of the 16 mm gap double glazing unit with aerogel only and with aerogel mixed with the maximum powder concentration. The transmittance reduction caused by the silica powder moderates the angular dependency; in fact, sample 3–1 solar transmittance drops by 0.22 from normal to 60 °C incidence, whereas the reduction is only 0.06 for sample 3–5. The same response is observed for the thicker samples with small deviations (0.19/0.20 and 0.04/0.05 for 0 % and 7.5 %, respectively).

4.2. Thermal properties

In continuity with the sample selection for optical properties, the thermal characterization focused on selected samples: namely samples 3 (16-mm gap thick), 4 (25-mm gap thick), and 5 (34-mm gap thick) with 0 %, 2 %, 4 %, and 7.5 % silica concentration were selected as more representative solutions. Table 6 reports the thermal resistance *R* and the thermal transmittance *U*. For each sample, 4 tests were conducted in steady-state conditions (surface temperatures and heat flux through the samples), setting the temperature (T_{test}) in the hot chamber at 45 °C and 50 °C. The relative uncertainties (type B), calculated according to [27], vary in the 2–5 % range for all the tests and they are within the measurement error of the device. U-values at 10 °C vary in the 1.04–0.92 W/m^{2}K (R = 0.79–0.92 m^{2}K/W), 0072–0.64 W/m^{2}K (R = 1.22–1.39 m^{2}K/W), 0.53–0.49 W/m^{2}K (R = 1.70–1.88 m^{2}K/W) ranges for the gap-thickness of the glazing systems of 16 mm, 25 mm, and 34 mm, respectively. As the percentage of silica powder increases, the thermal performance improves (Fig. 11). A higher reduction in thermal transmittance occurs with 4 and 7.5 % of silica powder, whereas only 2 % involves a minimal contribution (maximum difference of 1 %), regardless of the gap thickness. The reductions follow an almost linear trend (regression of 0.97 for 16-mm and 34-mm gap thick and of 0.92 for 25-mm gap thick). For the same mixture, the increase in the thickness of the gap leads to a reduction in thermal transmittance up to 30 % from 16 mm to 25 mm gap-thick and 27 % from 25 mm to 34 mm gap-thick.

4.3. Building energy performance analysis

Although the entire building was modelled, the results of a single intermediate floor are presented as an exemplary case. Fig. 12 shows the total yearly primary energy use for the different glazing configurations

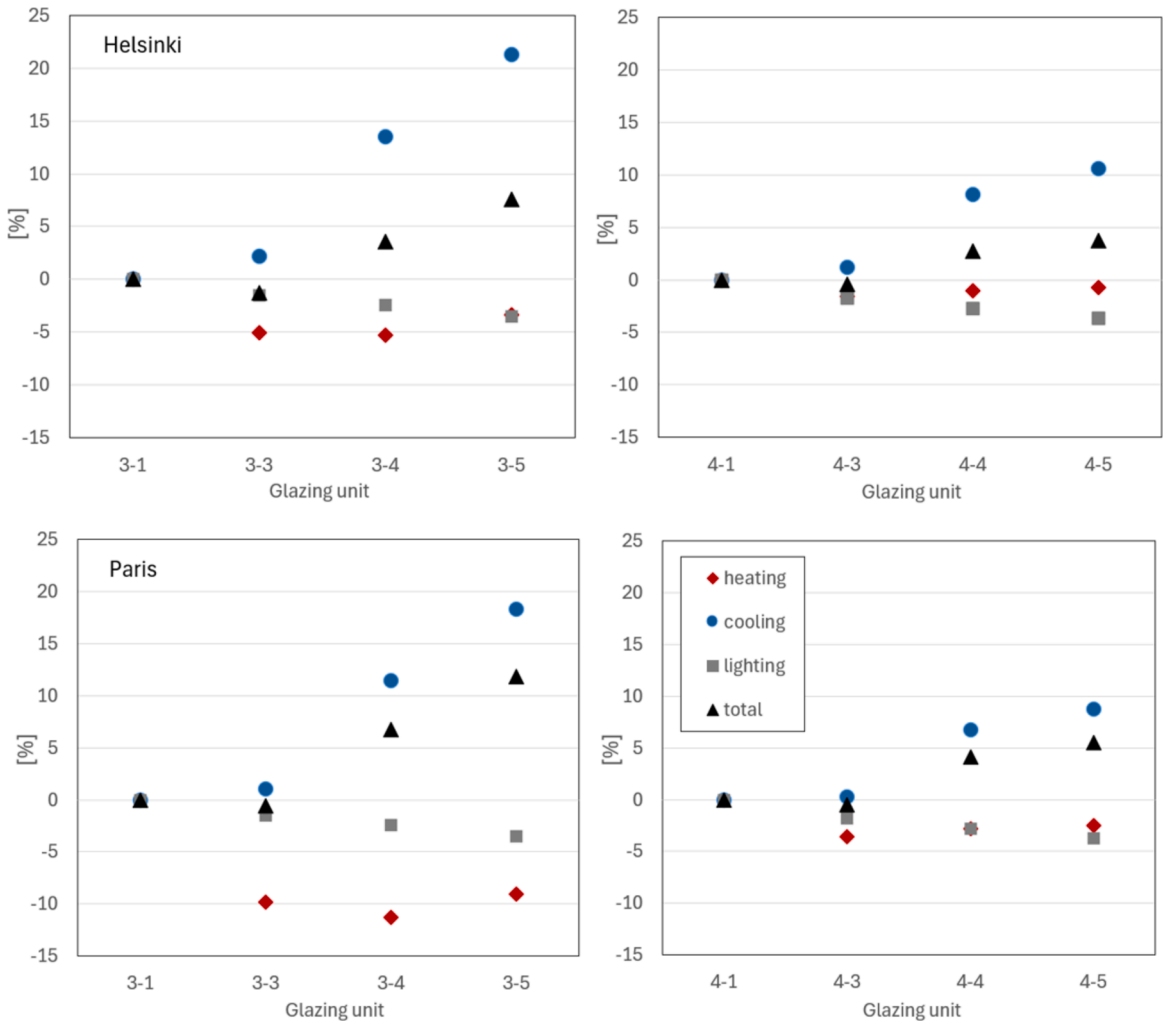

Fig. 13. Relative variations for heating, cooling, lighting, and total energy use in Helsinki and Paris.

and localities, disaggregated for heating, cooling, and lighting services. While the results for Helsinki exhibit a balanced use between heating and cooling, Paris and, as expected, Palermo are cooling-dominated; in addition, these two cities exhibit energy use for lighting almost identical. Due to these findings and for the sake of synthesis, only the Paris results are analysed, the ones about Palermo can be derived by analogy.

The first finding is related to the high energy use for cooling in both cities, despite their climatic conditions, which may be attributed to high internal gains and to the high solar gains of a fully glazed building. Concerning the impact of the aerogel glazing, it is observed that the 25 mm pane reduces the total energy use by 3.1 and 2.6 kWh/m^2 with respect to the 16 mm layer in Helsinki and Paris, respectively. The difference is due to the reduction of cooling use due to the lower solar gains; slight increase of heating use and negligible variations of electric lighting use are observed.

Going into the details of the impact of the aerogel powder, it is relevant to observe the relative variation of the energy use with respect to the no-silica powder samples in Helsinki and Palermo in Fig. 13, besides the absolute variations.

For sample 3 (16 mm aerogel thickness) in Helsinki, the maximum heating use increase is observed for the 4 % powder concentration and it is close to 2 kWh/m^2 (5 %) and there is not a defined trend as a function of the powder concentration. The cooling use is instead highly sensible to the powder concentration and the energy decreases accordingly, reaching 21 % (about 8.5 kWh/m^2) for 7.5 % powder. Lighting is inversely sensible to the powder concentration (as it reduces the light transmission), however, the penalty is below 0.5 kWh/m^2 per year. In terms of total energy use, 2 % silica powder slightly worsens the initial performance, while the 7.5 % powder reduces it by 7.6 % (close to 7 kWh/m^2). The 25 mm thick aerogel sample is intrinsically more efficient in terms of thermal insulation and solar control (lower transmittance): the variations caused by the silica powder are residual for heating and lighting uses (<1 kWh/m^2), but still relevant for the cooling use, peaking more than 10 % (4 kWh/m^2) for the 7.5 % sample. The total energy uses range from −0.4 % (2 % concentration) up to 3.8 % (3 kWh/m^2) for the sample 3–5.

The results of the reference floor for Paris exhibit a very strong predominance of cooling energy use, as the heating one accounts for about 15 % of the latter for the samples of both thicknesses. The absolute differences of heating and lighting uses are always lower than 1 kWh/m^2 for all powder concentrations with respect to the aerogel pane with no silica powder. The cooling savings reach 10 kWh/m^2 for samples 3–5 leading to 12 % total energy savings; it should to be noted that the 4 % silica powder provides 7 % total energy savings (>5 kWh/m^2). The absolute and relative savings get smaller with thicker samples. The 2 % concentration does not change the initial performance of the system; however, higher concentrations ensure cooling and total energy savings by 3–4 kWh/m^2, corresponding to 4–6 % in relative terms.

If the silica powder exhibits a significant impact on the lighting and solar parameters even in small concentrations, the same does not relate

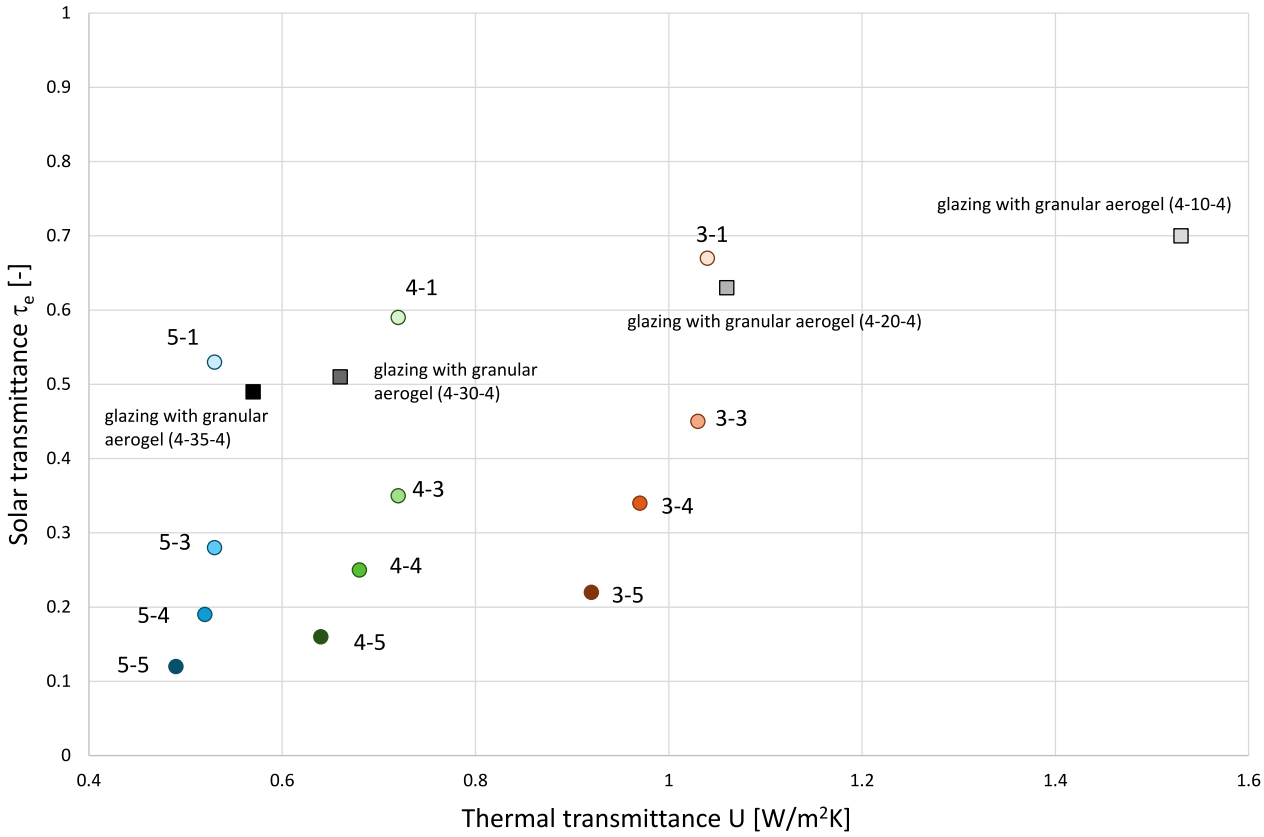

Fig. 14. Solar transmittance of the examined samples and data from literature vs the U-value.

to the application at the building scale. The effect of 2 % concentration almost negligible in terms of total energy use; higher concentrations ensure improved performance, especially in cooling dominate contexts.

5. Discussion

The optical properties of the investigated samples confirm the mainly transparent, yet diffusing, behaviour of the materials and the very low absorbance, especially in the visible range, in accordance with the existing literature. The transmittance spectra of the base-case systems (Fig. 7) show no differences in the profiles when increasing the material thickness and a moderate reduction in the transmission coefficient, that is at most 0.2 when passing from 7 to 34 mm. The introduction of silica powder in the granular aerogel gap does not cause any significant variations in terms of the spectral response of the glazing unit, as observed in Fig. 8 for the thinnest sample. The material has a small selectivity, with the transmittance and reflectance in the visible range a few digits greater than in the solar range, and this behaviour remains unchanged also with the introduction of the silica powder.

While no changes are observed on the profile of the spectra, the silica powder has, conversely, a strong impact on the absolute transmission levels, as inferred again from the transmittance spectra in Fig. 8 (16 mm gap sample for the different powder concentrations): a significant reduction is observed when adding only 1 % of powder (about 0.1). This reduction is approximately the same when the powder percentage increases from 2 to 4 % and from 4 to 7.5 %. A total reduction of about 0.5 is observed when adding 7.5 % of silica powder concerning the sample without powder. This behaviour is emphasized with higher thicknesses, whereby adding only 2 % of silica powder a 0.2 reduction is obtained; values lower than 0.2 are observed with the higher thickness and the higher powder percentage.

The change in transmittance and reflectance is intimately linked to the thickness of the samples when the powder is added, as proven by the off-normal transmittance measurements. It was in fact observed that the absolute difference of the normal and off-normal transmittance decreased with the increase of the sample thickness at the same concentration; such difference was instead negligible for the pure granular aerogel [2]. It can be explained by the fact that the higher the concentration, the lower the transmittance, thus the absolute differences get lower as well.

The combined observation of solar and thermal variations as a function of the silica powder concentration provides some interesting details, also reflected in the numerical analysis. While the solar transmittance, and thus the solar gains through the glazing system, progressively decreases with the increment of powder in the mixture, the thermal resistance (transmittance) does not substantially change for small concentrations (1–2 %) but progressively decreases (increases) with higher powder contents.

This behaviour of the solar transmittance vs. the thermal transmittance explains, consequently, the negative results achieved in Helsinki and Paris for the samples with 2 % concentration. In fact, such glazing configurations have a very limited impact on cooling and lighting performance but not on heating, whose consumption substantially increases. This can be explained by lower solar gains and invariance of thermal resistance, resulting in higher energy demand for the space heating system; at higher silica powder concentrations the lower solar gains are partly compensated by the higher thermal resistance, with the consequence that the heating energy uses are similar or lower than those achieved with the 2 % concentration. It must be also noted that with 4 % and 7.5 % powder concentration, a significant reduction of the cooling energy use is calculated.

In general, the 3–5 and 4–5 (7.5 % concentration) alternatives are the most effective with the overall lower energy demand for all the analysed locations. Given the substantial invariance of lighting needs due to the rather low artificial illumination activation threshold and the substantial satisfaction of the threshold also thanks to the predominance

of transparent surfaces, attention must be focused on the distribution of heating and cooling needs, as well as the relation between solar gains and thermal transmission gains/losses through the glazed envelope. As an example, in the selected building the best solution is the one with the lowest solar transmittance, case 3–5, whose value is very similar to that of case 4–4. However, the lower thermal resistance of the former, 0.92 W/m^2K compared to 0.68 W/m^2K, allows it to benefit from greater heat losses during the night, acting like a sort of pre-cooling the environment and consequently reducing the cooling demand. In this perspective the numerical analysis here carried out must be considered as a preliminary step. The effectiveness of the silica powder in improving the energy performance of buildings equipped with aerogel glazing should be explored for several variants, including the building use, the mix of reference heating/cooling lighting energy use, and the transparent area to total building envelope ratio.

A comparison with data from Literature was finally carried out, by evaluating the relationship between the solar transmittance τ_e and the thermal transmittance U (see Fig. 14). It can be observed that the samples investigated in the present study show a significant reduction in the solar transmittance when adding the silica powder; anyway, the powder percentage has less influence on the τ_e values. Conversely, a slight decrease in the thermal transmittance is observed when increasing the powder percentage. The samples without the powder are compared with data from [33], where the thermal and optical properties of aerogel samples with different granule sizes were investigated. Data related to samples with LA1000 are reported in Fig. 14, compared to the samples without powder studied in the present work. A similar trend is observed for the τ_e vs. U, despite slightly higher values of the solar transmittance are obtained for the samples here investigated, when considering the approximately the same thickness. It could be related to the improvement during the time of the transmission optical properties of the LA1000 granular aerogel.

6. Conclusion

Despite the thermal insulation properties of glazing systems equipped with transparent aerogel is a well-established technology to reduce space heating energy use in buildings, little explored is the way of modulating the solar gains through highly transparent aerogel façade to avoid overheating risks in buildings with relevant cooling demand and use. To this purpose, this study provides a detailed analysis, both experimental and numerical, of an innovative solution based on a mixture of granular aerogel with hollow silica powder to increase the reflectance of the glazing systems and, consequently, reduce the solar and lighting transmission.

A number of double glazing samples with the mixture in the gap were produced, different thicknesses and powder concentrations, the latter varying from 0 % to 7.5 %. The optical measurements proved that the solar and light transmittance can be reduced up to 0.48 and 0.45 on a 0–1 scale, respectively. Analogously, the solar and light reflectance can be increased up to 0.49 and 0.46, respectively. The silica powder also improves the thermal insulation performance of the system reducing the convection heat transfer, and the thermal resistance of a glazing system so conceived can increase to 0.18 m^2K/W, or improve by 10 % in relative terms.

Exemplary cases were also run in numerical exercise, in which the performance of an office building equipped with aerogel and silica powder façade was analyzed in a transient regime. The results showed that the lighting performance was loosely affected by the glazing configuration, due to the high glazing surface; the space heating use was moderately affected by the difference configurations, mainly because of the antagonist impact of lower solar gains and higher thermal insulation. The greatest benefits were found for cooling energy use, with savings of up to 21 %. Due to the high cooling demand and use of the selected building, the impact of the silica powder was positive for high concentration (4 % and 7.5 %), ensuring total energy savings up to 12 %.

This study thus demonstrates the benefits of hollow silica powder to be added to transparent granular aerogel windows and façades in buildings with relevant cooling demand. However, more analyses are needed to explore in detail the (day) lighting aspects and the energy performance of buildings with higher heating use, to have a complete framework for the potential of the selected technology.

CRediT authorship contribution statement

F. Merli: Writing – original draft, Software, Methodology, Investigation, Formal analysis. **C. Buratti:** Writing – original draft, Supervision, Methodology, Investigation, Data curation, Conceptualization. **T. Ihara:** Writing – review & editing, Supervision, Methodology. **A.G. Mainini:** Writing – original draft, Software, Methodology, Formal analysis. **A. Augello:** Visualization, Software, Formal analysis. **M. Zinzi:** Writing – original draft, Validation, Methodology, Investigation, Conceptualization.

Declaration of competing interest

The authors declare that they have no known competing financial interests or personal relationships that could have appeared to influence the work reported in this paper.

Data availability

Data will be made available on request.

Acknowledgements

This study was partly developed in the framework of the research activities carried out within the Project “Network 4 Energy Sustainable Transition — NEST”, Spoke 8: Final use optimization, sustainability \& resilience in energy supply chain, Project code PE0000021, Concession Decree No. 1561 of 11.10.2022 adopted by Ministero dell’Università e della Ricerca (MUR), CUP ENEA I83C22001800006, Project funded under the National Recovery and Resilience Plan (NRRP), Mission 4 Component 2 Investment 1.3 - Call for tender No. 341 of 15.03.2022 of Ministero dell’Università e della Ricerca (MUR); funded by the European Union – NextGeneration EU.“

References

[1] M. Santamouris, K. Vasilakopoulou, Present and future energy consumption of buildings: Challenges and opportunities towards decarbonisation. e-Prime – Adv. Electr. Eng. Electron. Energy 1 (2021) 100002 https://doi.org/10.1016/j.prime.2021.100002.
[2] C. Buratti, E. Belloni, F. Merli, M. Zinzi, Aerogel glazing systems for building applications: A review, Energ. Buildings 231 (2021) 110587, https://doi.org/10.1016/j.enbuild.2020.110587.
[3] C. Buratti, E. Moretti. Nanogel windows, in: F.P. Torgal, M. Mstretta, A. Kaklauskas, C.G. Granqvist, L.F. Cabeza (Eds.), Nearly zero energy building refurbishment, A multidisciplinary approach, Springer, London, 2013, pp. 555–581.
[4] H. Wang, H. Wu, Y. Ding, J. Feng, S. Wang, Feasibility and optimization of aerogel glazing system for building energy efficiency in different climates, Int. J. Low-Carbon Technol. (2014) 1–8.
[5] C. Buratti, E. Moretti, M. Zinzi, High energy-efficient windows with silica aerogel for building refurbishment: Experimental characterization and preliminary simulations in different climate conditions, Buildings 7 (2017) 1–12.
[6] C. Buratti, E. Moretti, E. Belloni, M. Zinzi, Experimental and numerical energy assessment of a monolithic aerogel glazing unit for building applications, Appl. Sci. 9 (2019) 5473.
[7] J.M. Schultz, K.I. Jensen, F.H. Kristiansen, Super insulating aerogel glazing, Sol. Energy Mater. Sol. Cells 89 (2–3) (2005) 275–285.
[8] J.M. Schultz, K.I. Jensen, Evacuated aerogel glazings, Vacuum 82 (7) (2008) 723–729.
[9] N. Lolli, I. Andresen, Aerogel vs. argon insulation in windows: A greenhouse gas emission analysis, Build. Environ. 101 (2016) 64–76.
[10] U. Berardi, Aerogel-enhanced systems for building energy retrofits: Insights from a case study, Energy Build. 159 (2018) 370–381.

[11] E. Field, A. Ghosh, Energy assessment of advanced and switchable windows for less energy-hungry buildings in the UK, Energy 283 (2023) 128999, https://doi.org/10.1016/j.energy.2023.128999.
[12] A.R. Hassani, P. Domenighini, E. Belloni, T. Ihara, C. Buratti, Evaluation of the solar heat gain coefficient of innovative aerogel glazing systems: Experimental campaigns and numerical results, J. Build. Eng. 62 (2022) 105354, https://doi.org/10.1016/j.jobe.2022.105354.
[13] Y. Xiaoyue, T. Llewellyn, Y. Siegfried, Investigations into impacts of fenestration and shading variation on ventilation and energy performance of an office in cooling and heating seasons, Sol. Energy 276 (2024) 112646.
[14] Y. Ming, Y. Sun, X. Liu, X. Liu, Y. Wu, Thermal performance of an advanced smart fenestration systems for low-energy buildings, Appl. Therm. Eng. 244 (2024) 122610.
[15] A.M. Qahtan, S. Shaik, Y.A. Alwadai, S. Alhamami, A.S. Alawlaki, M.H. Alyami, J. A. Kodati, Smart glazing systems vs conventional glazing: a comprehensive study on temperature control, daylighting, and sustainability, Int. J. Sustain. Dev. Plan. 19 (3) (2024) 939–947.
[16] M.T. Naqash, Analyzing glass configurations for energy efficiency in building envelopes: a comparative study, J. Appl. Sci. Eng. 28 (2) (2023) 319–333.
[17] F. Merli, M. Zinzi, C. Buratti, A. Augello, T. Ihara. Thermal and Optical Performance of Advanced Polycarbonate Systems with Granular Aerogel and Hollow Silica Powder. Proceedings 5th International Conference on Building Energy and Environment COBEE 2022, Montreal (Canada), July 25-29, 2022. In: Springer Nature Singapore. https//doi.org/10.1007/978-981-19-9822-5_74.
[18] E. Belloni, C. Buratti, F. Merli, E. Moretti, T. Ihara, Thermal-energy and lighting performance of aerogel glazings with hollow silica: Field experimental study and dynamic simulations, Energ. Buildings 243 (2021) 110999, https://doi.org/10.1016/j.enbuild.2021.110999.
[19] H. Begum, Y. Xue, J. S. Bolton, K. V. Horoshenkov. A key physical mechanism that controls the sound absorption of aerogel powders. Inter-Noise 2022, Glasgow (UK), August 2022.
[20] A. Maccari, M. Montecchi, F. Treppo, M. Zinzi, CATRAM: an apparatus for the optical characterization of advanced transparent materials, Appl. Opt. 37 (1998) 5156–5161.
[21] EN 410. Glass in building – Determination of luminous and solar characteristics of glazing, 2011.
[22] C. Buratti, E. Belloni, L. Lunghi, M. Barbanera, Thermal conductivity measurements by means of a new 'small hot-box' apparatus: manufacturing, calibration and preliminary experimental tests on different materials, Int. J. Thermo- Phys. (2016) 37–47.
[23] EN ISO 8990:1996. Thermal Insulation—Determination of Steady State Thermal Transmission Properties—Calibrated and Guarded Hot Box. ISO: Brussels, Belgium, 1996.
[24] ISO 10456:2007. Building Materials and Products—Hygrothermal Properties—Tabulated Design Values and Procedures for Determining Declared and Design Thermal Values. ISO: Geneva, Switzerland, 2007.
[25] C. Buratti, F. Merli, E. Moretti, Aerogel-based materials for building applications: Influence of granule size on thermal and acoustic performance, Energ. Buildings 152 (2017) 472–482.
[26] UNI EN ISO 6946:2008. Building components and building elements - Thermal resistance and thermal transmittance - Calculation method.
[27] JCGM 100, GUM 1995 with minor corrections evaluation of measurement data—guide to the expression of uncertainty in measurement (2008).
[28] Integrated Environmental Solutions Limited. 2023. IES Virtual Environment (Version 2023)- computer software. Available on http://www.iesve.com.
[29] G. Ward, R. Mistrick, E.S. Lee, A. McNeil, J. Jonsson, 2023. Radiance (Version 5.4) - computer software. Retrieved from https://radiance-online.org/.
[30] C.F. Reinhart, J. Mardaljevic, Z. Rogers, Dynamic daylight performance metrics for sustainable building design, LEUKOS – J. Illumin. Eng. Soc. N. Am. 3 (1) (2006) 7–31.
[31] Meteonorm. (Version 8.0.3.15910). Meteonorm: Global weather data for renewable energy. Retrieved from https://meteonorm.com/en/.
[32] ISO 18523-1:2016. Energy performance of buildings — Schedule and condition of building, zone and space usage for energy calculation — Part 1: Non-residential buildings.
[33] E. Moretti, E. Belloni, F. Merli, M. Zinzi, C. Buratti, Laboratory and pilot scale characterization of granular aerogel glazing systems, Energ. Buildings 202 (2019) 109349.